Atmos. Chem. Phys., 5, 2949–2959, 2005
www.atmos-chem-phys.org/acp/5/2949/
SRef-ID: 1680-7324/acp/2005-5-2949
European Geosciences Union

Atmospheric Chemistry and Physics

High-precision isotope measurements of $H_2^{16}O$, $H_2^{17}O$, $H_2^{18}O$, and the $\Delta^{17}O$-anomaly of water vapor in the southern lowermost stratosphere

P. Franz and T. Röckmann

Max-Planck-Institute for Nuclear Physics, Heidelberg, Germany

Received: 6 April 2005 – Published in Atmos. Chem. Phys. Discuss.: 28 July 2005
Revised: 20 October 2005 – Accepted: 21 October 2005 – Published: 7 November 2005

Abstract. We report the first high-precision measurements of $\delta^{18}O$ and $\Delta^{17}O$ at high southern latitudes that can resolve changes in the isotopic composition of water vapor in the lowermost stratosphere and upper troposphere. A strong increase of $\delta^{18}O$ with decreasing mixing ratio above the tropopause is evident in the data. Since also the water vapor mixing ratio decreases above the tropopause, the effect seen in the isotope data can be explained by mixing of moist air from the tropopause with dry stratospheric air. However, the source of this dry stratospheric air is not known; both fast transport from the extratropical tropopause or mixing with air from the dehydrated polar vortex are likely. The magnitude of the $\Delta^{17}O$-anomaly (departure from mass-dependent fractionation (MDF)) was below 2 per mil for each datapoint, and a zero anomaly in lower level stratospheric water vapor is possible. Various transport histories for the stratospheric data are discussed based on the mixing ratio and isotope data.

1 Introduction

Water vapor is an important player in many atmospheric processes. In the troposphere, its most important features are clouds, precipitation and its role as a greenhouse gas. For atmospheric chemistry, reaction of H_2O with electronically excited oxygen atoms $O(^1D)$ provides the main source of hydroxyl radicals, which are responsible for the self-cleansing ability of the atmosphere. Air entering the stratosphere contains only $\sim 3-4$ ppm H_2O due to the very cold tropopause temperatures. Inside the stratosphere, an additional $\sim 1-2$ ppm are produced by methane oxidation. The OH radicals stemming from H_2O play a role for example in ozone chemistry and CH_4 decomposition. Further, inside the polar vortex, polar stratospheric cloud (PSC) particles are formed at low temperatures from water vapor and nitric and sulfuric acids. Heterogeneous chemistry on the surface of these PSC particles enable the transfer of inactive chlorine compounds into active ones, which is a major prerequisite for the occurence of the polar ozone hole in polar spring. Thus the stratosphere is very sensitive to changes in water vapor concentrations (Kirk-Davidoff et al., 1999; Forster and Shine, 2002; Stenke and Grewe, 2005).

Despite its important role in the stratosphere, the pathways by which water enters the stratosphere, and how its mixing ratio is altered by photochemistry, are poorly understood. An alarming aspect is that water vapor concentrations may have risen by ∼50% in the stratosphere over the last 50 years (Oltmans et al., 2000; Rosenlof et al., 2001), though the reasons are not clear. About half of this increase may be directly due to increased methane concentrations. For the remaining amount, different theories are under discussion. Röckmann et al. (2004) suggested that the oxidation capacity of the stratosphere might have increased due to elevated chlorine and water vapor levels, leading to a more efficient methane decomposition in the upper stratosphere. In the lower stratosphere, changes in global circulation patterns, like a widening of the convective updraft zone in which water vapor enters the stratosphere, may be the cause for increased water vapor levels (Rosenlof, 2002).

It is believed that isotope measurements can give valuable additional information to distinguish between processes controlling the water vapor budget of the stratosphere. This is mainly due to the fact that isotopically substituted molecules have different water vapor pressures and reaction rates than the unsubstituted molecules. For example, heavy water molecules are preferentially removed in condensation, leading to a drastic heavy isotope depletion of atmospheric water vapor at tropopause level. Since ∼99% of all photochemically produced water stems from H-abstraction by OH, changes in the oxygen isotopic composition of water vapor can directly be linked to the important hydroxyl radical.

Correspondence to: P. Franz
(p.franz@niwa.co.nz)

Isotopic abundances of water isotopologues are usually expressed in the δ-notation,

$$\delta X = \left(\frac{R_{\text{sample}}}{R_{\text{VSMOW}}} - 1 \right) \cdot 1000‰ \quad (1)$$

where X in the case of water denotes either D (deuterium), ^{17}O or ^{18}O; R is the ratio of heavy/light isotope (e.g. $[^{17}O]/[^{16}O]$). Since δ-values are usually small they are expressed per mil (‰), thus the numerical value of 1‰ equals 0.001. R_{VSMOW}=2005.20$\cdot 10^{-6}$ is the internationally accepted isotope standard ratio for ^{18}O of Vienna Standard Mean Ocean Water.

In natural liquid water reservoirs, a tight relationship between ^{17}O and ^{18}O exists as changes in δ^{18}O are approximately twice as large as changes in δ^{17}O (Miller, 2002; Meijer and Li, 1998). This relationship is referred to as mass-dependent fractionation (MDF). Deviation from this behavior is called Δ^{17}O-anomaly or mass-independendent fractionation (MIF), and can be quantified in the form

$$\Delta^{17}O = \left(\ln(1+\delta^{17}O) - 0.528 \cdot \ln(1+\delta^{18}O) \right) \cdot 1000‰ \quad (2)$$

Since the isotopic composition of water vapor in the troposphere is dominated by mass-dependent effects like evaporation and condensation, it is expected to have a zero Δ^{17}O-anomaly. However, this may change in the stratosphere. Here the isotopic composition of water vapor is controlled by photochemistry. In principle, this also follows mass-dependent fractionation rules. However, in these reactions small deviations from the proportionality factor 0.528 occur (Young et al., 2002), since each chemical reaction has its own proportionality factor. This is primarly caused by different reduced masses, leading to lower collision rates for heavier molecules. This effect can lead to a small intrinsic Δ^{17}O anomaly in water vapor. In addition, a large anomaly of up to ∼30‰ could be introduced by isotope exchange between NO_x, which inherits a strong anomaly from ozone, and H_2O, though the rate constant for this process still has to be experimentally quantified (Lyons, 2001). On the other hand, isotope exchange with also unknown reaction rates between HO_2, OH and O_2 could diminish mass independent fractionation in OH and H_2O (Lyons, 2001). Therefore, these rate constants have to be known in order to successfully model the oxygen isotopic composition of stratospheric water vapor.

Over the last 4 decades, significant effort has been put into the task of measuring the stable isotopologues of water vapor (Abbas et al., 1987; Carli and Park, 1988; Dinelli et al., 1991, 1997; Guo et al., 1989; Johnson et al., 2001; Kuang et al., 2003; Moyer et al., 1996; Pollock et al., 1980; Rinsland et al., 1991; Stowasser et al., 1999; Webster and Heymsfield, 2003; Zahn et al., 1998). The precisions in these studies were usually larger than 20‰ for δD. This is sufficient to investigate the strong variability of δD in the atmosphere. In particular the recent study of Webster and Heymsfield (2003) showed isotope signals inside and outside of clouds with high temporal resolution, which can be used to determine cloud origins.

For δ^{18}O, analytical errors are typically not better than ∼70‰. Only the measurements of Zahn et al. (1998) in the upper troposphere have better precisions for δ^{18}O of ∼3−7‰. As models of δ^{18}O do not predict atmospheric changes larger than ∼120‰, high precision is necessary to detect the atmospheric isotope variations above the analytical error (Franz, 2005). No study so far has been able to investigate the Δ^{17}O anomaly with sufficient precision, where only variations of a few permil have been predicted by models.

Cryogenic water samplers so far have been used in combination with traditional "offline" methods for conversion of H_2O to H_2 and O_2 for mass-spectrometric analysis. Since these offline methods require quite large sample amounts (typically 100 mg water), huge air volumes have to be sampled as the water vapor mixing ratio of the stratosphere is low. Therefore, large traps are necessary to allow efficient trapping of water vapor at high flowrates of air. Associated with the large size of the traps are large surface areas, which are hard to clean from adsorbed water molecules, and therefore display significant memory effects (Zahn, 1995; Zahn et al., 1998). The sampler used in this work makes use of an online method described in Franz and Röckmann (2004), which reduces the required sample amount to less than 100 μg. The corresponding traps are small (∼150 ml) and can be purged easily, thus minimizing memory effects. Pollock et al. (1980) used similar sample amounts, but measured HDO and HTO (tritiated water vapor) only.

The new analytical system allows in principle to measure δD, δ^{18}O, δ^{17}O and the water vapor mixing ratio υ. However, due to some problems with the deuterium measurements at the time of analysis of our samples, only the ^{17}O and ^{18}O substituted isotopologues could be analyzed. In this paper, we present the first real high-precision measurements of δ^{18}O and Δ^{17}O on water vapor from the lower stratosphere. The 1σ-error of δ^{18}O is typically 3−4‰. Due to a very tight relationship between δ^{17}O and δ^{18}O of individual samples, the error of Δ^{17}O is typically 0.3‰ for sample sizes of 100 μg, and 2‰ for the smallest samples of ∼20 μg. Only with these precisions can the structures in the stratospheric profiles of δ^{18}O and Δ^{17}O be resolved.

2 Instrumental setup

The details of the instrumental setup are described elsewhere (Franz and Röckmann, 2004; Franz, 2005), so that only a brief overview will be given here.

Samples are collected in custom-made stainless steel vessels with gold-plated inner surface and 150 mL internal volume. Up to ten vessels are mounted into a dewar containing liquid nitrogen and are attached to a electropolished stainless steel manifold. Before sampling, the sample containers are purged individually at 250°C in a clean He-stream prior to

attaching them to the sampling system. Prior to sampling, the inlet manifold of the sampling unit is heated to about 150°C and evacuated for at least 12 h.

During sampling, a mass-flow of 300 ccm/min (STP) is let through the sampling tubes, controlled by a mass-flow controller. A small stainless steel frit of 20 μm pore size prevents small ice crystals from being flushed out of the sample container. Normal sampling time is around 20 min, though longer times are needed for lower water vapor mixing ratios at high altitudes.

Since not only H_2O but also CO_2 is frozen out at liquid nitrogen temperature, the sample H_2O has to be separated from the carbon dioxide. Isotope exchange between CO_2 and liquid H_2O would greatly affect the results. Therefore, after sampling the liquid nitrogen in the dewar is replaced with acetone ice. Each sample container is evacuated individually at temperatures between −95°C and −110°C until a pressure of $\sim 5 \cdot 10^{-3}$ hPa is reached, hence only keeping H_2O in the container.

For sample analysis, a sample container is connected to the analytical system and heated to 250°C. The connecting dead volumes are first thoroughly evacuated to 10^{-2} hPa, and flushed with He to prevent contaminations. Then the sample is flushed from the container into the analytical system in a He stream via a heated line. From each sample, subsequently ten aliquots are frozen out in a liquid nitrogen cooled cryotrap. The aliquots are released by heating the trap to 400°C into a tube filled with CoF_3, which converts the H_2O to O_2, HF and CoF_2. Further traps of NaF and liquid nitrogen ensure that only the O_2 product reaches an open split interface, from where the sample aliquots are admitted to the mass spectrometer (Delta-Plus XP, Finnigan).

From the time-series of the aliquots, the machine-response of the sample is determined as described in Franz and Röckmann (2004). Since the machine response is not the true isotopic composition of the sample, a calibration is mandatory. For this, a calibration line has been built that is capable of producing water vapor with known mixing ratio and isotopic composition. In this calibration line, two small nitrogen gas streams (between 0 and 7 ccm/min) are directed through two bubblers containing two water reservoirs with very different isotopic composition. After passing through the bubblers, the gas streams have 100% relative humidity. The isotopic composition of the gas phase is in equilibrium with the liquid phase, and is fractionated with well-known fractionation constants; details can be found in Franz (2005). Behind the bubblers, the gas streams are combined in a large nitrogen stream (1200 ccm/min) with zero water content. In this fashion, gas streams with mixing ratios between 0 and 60 ppm can be obtained. The isotopic composition is determined by controlling the two flow rates through the bubblers, and can be set between δ^{18}O=−19.6...−59.6‰. Further, CO_2 can be added to simulate the CO_2 separation process. The isotope calibration is performed with the real sampling system.

The precision of the entire system is determined by the analytical system, the calibration, blanks and a 10% memory effect consideration between samples. Typical 1σ errors in δ^{18}O are about 2−3‰, and 1.5−2‰ in δ^{17}O. However, due to a very tight correlation between individual samples, Δ^{17}O can be determined with precisions between 0.3 and 2‰, depending on sample amount (Franz, 2005; Franz and Röckmann, 2004).

The calibration system can also be used to calibrate the H_2O mixing ratio measurement, because known amounts of water can be collected and retrieved back from the sample containers. The integrated peak area of an unknown sample is then compared to the peak area from samples obtained from the calibration line, where the mixing ratio is known. Knowing the amount of air collected, the mixing ratio can thus be easily calculated. It was later discovered that one mass flow controller in the analytical system suffered from voltage fluctuations, leading to an uncertainty of 20% in the mixing ratio calibration, though the isotope measurements were not affected by this problem.

3 Sample measurements

Using the analytical equipment described above, isotope measurements on upper tropospheric and stratospheric water vapor were made on samples collected on aircraft flights between New Zealand and Antarctica. The aircraft, a C-17 Globemaster, operates as a transporter for staff and equipment for the Antarctic observatories McMurdo and Scott Base. These aircraft are not designed for, but are frequently used for scientific experiments.

The sampling region was chosen for two main reasons. First, the tropopause level is located at lower altitudes near the poles, and thus it is possible to sample stratospheric air without making use of special high altitude aircraft. Second, one of the main goals of the work presented here was to quantify the Δ^{17}O anomaly in stratospheric water vapor. As global circulation results in downward flux of older stratospheric air at high latitudes (Rosenlof, 1995), the probability to find an isotope anomaly is higher near the poles.

Overall, four flights were performed; two in August and two in October 2004. The sample inlet was connected to the hull of the aircraft, with its inlet/outlet slits located at a minimum distance of ∼15 cm from the aircraft hull and before the wing and engines. Since this is not a scientific flight, navigational data were not measured online and so data that were written down by the aircraft crew at intervals of ∼30 min have to be used. From these data the position, temperature and altitude of the samples collected are interpolated. As the airplane is kept at a stable level through most of the flight, these interpolations are sufficiently accurate.

The tropopause heights are derived from potential vorticity plots received from the NASA Goddard Automailer, which are available every 24 h. Due to limited resolution, the error

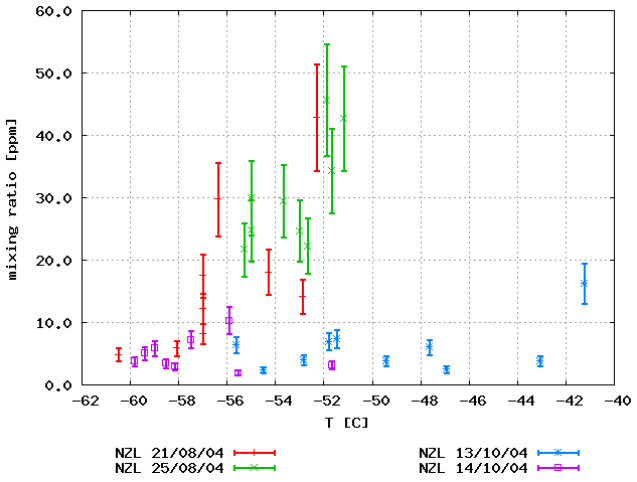

Fig. 1. H_2O-mixing ratio plotted versus ambient temperature. The samples can clearly be separated into stratospheric samples with υ<10 ppm, and samples from the tropopause region, which still show a temperature dependence.

in locating the tropopause at −1.6 potential vorticity units is estimated at 800 m.

Samples for the analysis of $\delta^{17}O$ and $\delta^{18}O$ were collected during flights on 21 and 25 August, and 13 and 14 October of 2004; dates, positions and isotopic data of the individual samples can be found in Table 1. Overall, 38 samples and 2 blanks were taken. The blanks were processed exactly like the samples (purging, heating, evacuating, freezing and transport). All samples were analyzed within 3 weeks after sampling to avoid chemical alteration in the sample containers as much as possible. Analysis was carried out as described above.

To avoid contamination with surface water from the inlet tube or the 3.5 m long flexible stainless steel line connecting the inlet to the sampler, the inlet line was flushed 30 min prior to sampling. The purge flow of >100 L/min (STP) provided by the dynamic forward pressure of the aircraft was maintained during the whole sampling process. Additionally, the inlet line had been flushed with dry nitrogen gas one day prior to each flight to remove surface water. These measures were taken to assure that the smaller air flow of 550 ccm/min (a sample flow of 300 ccm/min plus a bypass flow) taken from the main flow into the sampler was free from surface contamination as far as possible.

The peak area of the blank taken in August was about 3−10% of a typical sample peak area. This introduces a minor error into most of the measurements. A check of the analytical system after the blank measurement revealed a minor blockage in one line, so that purging the sample containers prior to sampling in August had been less effective than it had been during the calibration. As repairing the lines was not an option (it might have affected the calibration), the sample containers were additionally evacuated after the purging procedure and refilled with helium after the measurement process. The blank taken in October was negligibly small, so that the line blockage can be identified as the source for the first background blank. To consider the blank in the samples taken in August, it is assumed that its isotopic composition stems from filling the containers via the calibration system, and the error is calculated accordingly with its isotopic range (i.e. $\delta^{18}O_{min}$=−59.6‰, $\delta^{18}O_{max}$=−19.6‰).

The combined errors are usually less than 2.5‰ and 5.0‰ for $\delta^{17}O$ and $\delta^{18}O$, respectively. Only the combination of small sample amount and high blank results in higher errors; one datapoint has been removed in the plots shown for this reason. The individual errors come to approximately 40% from the error introduced by the isotope calibration and 40% from the high blank in the measurements of August; the remaining 20% of the error comes from memory effects. As the blank is zero in the October measurements, approximately two thirds of the error in these data come from the calibration, and one third from the memory effects.

4 Results and discussion

4.1 Water vapor mixing ratios

In Fig. 1 the H_2O mixing ratio is plotted versus ambient temperature. We found values between 2 and 50 ppm. These low mixing ratios indicate the absence of strong contamination during sampling or from the sampling containers. For air crossing the tropopause from the troposphere, the tropopause cold point determines the last point at which condensation can occur. Therefore, a correlation between tropopause temperature and mixing ratio is expected at tropopause level or below (Zahn et al., 1998; Zahn, 2001). Such a dependence, though with a high scatter, is seen for samples with υ>10 ppm in Fig. 1. Neglecting the outlier at −41°C, a gradient of ∼4 ppm/°C is found.

Air above the tropopause cold point is subject to temperature changes without additional condensation events, so that water vapor above the cold point has already lost some of its temperature history. Therefore, the correlation between the mixing ratio of water vapor and temperature is lost in the stratosphere, and the scatter of a plot versus temperature above tropopause level increases, and is further enhanced by mixing with stratospheric air (Zahn et al., 1998). Since there is no correlation between ambient temperature and mixing ratio in the data for υ<10 ppm, samples below 10 ppm are from hereon classified as “stratospheric”, whereas samples with mixing ratios above 10 ppm are labeled “tropopause”, i.e. to be strongly influenced by the tropopause temperature. More accurately, the “stratospheric” samples stem from the lowermost stratosphere. Only three samples of the first flight in August belong to the stratospheric dataset. These three samples all were taken at latitudes of 65 degrees south and

Table 1. Data of the $\delta^{17}O$, $\delta^{18}O$ measurements. Tropopause levels (alt.tp.) are obtained from the NASA Goddard Automailer. Errors are 1σ errors. Additional data can be found in Franz (2005), or can be directly obtained from the authors.

no	date [Z]	long. [degr]	lat. [degr]	T [C]	alt. [m]	alt.tp. [m]	υ [ppm]	$\pm$ [ppm]	$\delta^{17}O$ [‰]	$\pm$ [‰]	$\delta^{18}O$ [‰]	$\pm$ [‰]	$\Delta^{17}O$ [‰]
1	21 Aug. 2004	171.15	−51.05	−52.3	8839	9000	42.9	8.5	−33	3.6	−60.9	6.7	−0.4
2	21 Aug. 2004	170.86	−53.92	−52.9	8839	8962	14.2	2.8	−30	2.6	−56.1	4.7	0.1
3	21 Aug. 2004	170.48	−56.62	−54.3	8839	8615	18.1	3.6	−25.4	1.8	−47.7	3.2	0
4	21 Aug. 2004	170.24	−59.11	−56.4	8839	8346	29.8	5.9	−37.2	2.3	−70.1	3.6	0.4
5	21 Aug. 2004	169.9	−61.77	−57	8839	8462	17.5	3.4	−42.3	3.4	−78.6	6.1	−0.1
6	21 Aug. 2004	169.31	−64.49	−57	8839	8538	12.3	2.4	−34	3.6	−61.3	6.1	−1.2
7	21 Aug. 2004	168.68	−67.15	−57	8839	8115	8.2	1.6	−26.4	3.9	−46.2	6.1	−1.8
8	21 Aug. 2004	168.07	−69.74	−58.1	9009	7231	5.9	1.2	−20.5	3.9	−35.7	8.1	−1.5
10	21 Aug. 2004	166.26	−74.52	−60.5	8956	7346	4.9	1	−17.8	6.1	−30.2	12.7	−1.8
11	25 Aug. 2004	171.24	−49.33	−53	8534	8570	24.7	4.9	−16	2.1	−29	3.9	−0.7
12	25 Aug. 2004	171.03	−50.95	−52.7	8534	8453	22.3	4.4	−16.7	1.5	−30.2	2.8	−0.6
13	25 Aug. 2004	170.64	−54.1	−51.9	8534	8181	45.7	9	−37.6	2.7	−69.8	3	−0.2
14	25 Aug. 2004	170.44	−56.5	−51.2	8534	8563	42.8	8.4	−43.1	2	−80.5	3.5	0.3
15	25 Aug. 2004	170.3	−58.46	−51.7	8646	8830	34.4	6.8	−35.8	1.9	−65.3	3.2	−0.8
16	25 Aug. 2004	170.14	−60.37	−53.7	8949	8828	29.5	5.8	−29.6	1.7	−54.6	2.8	−0.4
17	25 Aug. 2004	169.83	−62.32	−55	9139	8442	24.8	4.9	−33.3	2	−61.9	3.6	−0.2
18	25 Aug. 2004	169.43	−64.33	−55	9144	7709	30	5.9	−34.4	1.8	−64.1	3.3	0
19	25 Aug. 2004	169.02	−66.35	−55.3	9144	7400	21.7	4.3	−30.6	2	−56.3	3.5	−0.5
20	13 Oct. 2004	171.36	−50.62	−41.23	8265	7269	16.3	3.2	−40.9	4.3	−76.9	8.1	0.5
21	13 Oct. 2004	171.06	−53.32	−43.09	8549	7000	3.9	0.8	−23.5	2.1	−47.1	2.1	1.7
22	13 Oct. 2004	170.79	−56.13	−47.67	8811	6808	6.1	1.2	−21.5	1.1	−43	2	1.5
23	13 Oct. 2004	170.41	−59.27	−51.48	8839	6885	7.4	1.5	−27.8	1.3	−54.1	2.2	1.2
24	13 Oct. 2004	169.94	−62.42	−51.81	8839	6346	7	1.4	−33.8	1.4	−64.4	2.4	0.7
25	13 Oct. 2004	169.41	−65.38	−52.86	8839	5769	4	0.8	−21.2	1.6	−42.1	2	1.3
26	13 Oct. 2004	168.7	−68.43	−55.63	8839	6346	6.5	1.3	−31.4	1.6	−59.8	2.3	0.7
27	13 Oct. 2004	168.83	−67.66	−54.52	10668	6115	2.4	0.5	−24.5	1.3	−45.4	2	−0.3
28	13 Oct. 2004	170.09	−61.44	−49.42	10668	6654	3.9	0.8	−11.8	1.6	−25.6	1.7	1.8
29	13 Oct. 2004	170.83	−55.61	−46.95	10668	6846	2.5	0.5	−13.5	1	−27.4	1.7	1.1
30	14 Oct. 2004	171.07	−53.26	−51.67	8839	6875	3.2	0.6	−25.1	2.7	−47	5.1	0
31	14 Oct. 2004	170.17	−60.88	−57.52	8992	7828	7.3	1.4	−40.2	2.1	−77	2.7	1.3
32	14 Oct. 2004	170.67	−57.09	−55.94	8839	7524	10.4	2.1	−47.7	1.7	−90.2	3	1.1
33	14 Oct. 2004	169.57	−64.55	−59.01	9144	7440	5.9	1.2	−41.6	1.6	−78.6	2.7	0.7
34	14 Oct. 2004	168.82	−67.83	−59.42	9144	6975	5.1	1	−38.1	1.4	−73.6	2.6	1.5
35	14 Oct. 2004	167.9	−71.13	−58.55	9144	6972	3.5	0.7	−28.6	1.5	−53.8	2.2	0.2
36	15 Oct. 2004	169.11	−66.28	−59.83	9449	7169	3.8	0.7	−34.3	1.4	−64.6	2.4	0.3
37	15 Oct. 2004	170.17	−60.54	−58.16	9449	7905	3	0.6	−35.3	1.3	−64.8	2.4	−0.6
38	15 Oct. 2004	170.92	−54.6	−55.55	9449	7142	2	0.4	−30.8	1.3	−56.2	2.2	−0.8

higher, where the tropopause is located at lower altitudes. No samples of the second flight in August are classified to belong to the stratospheric subset.

Figure 2 shows the measured H_2O mixing ratios plotted versus the distance to the tropopause. The "tropopause" samples show a scatter between 10…50 ppm, though no dependence on the distance to the tropopause is seen. The stratospheric samples show a decrease in mixing ratio with increasing distance to the tropopause, until pure stratospheric mixing ratios are encountered. Some of the datapoints actually reach mixing ratios lower than the typical stratospheric range of ∼4...6 ppm. Since the difference from this stratospheric mixing ratio range is statistically significant, the stratospheric air must have undergone further dehydration, or could have mixed with the dehydrated polar vortex. Especially the samples taken in October are very dry, whereas

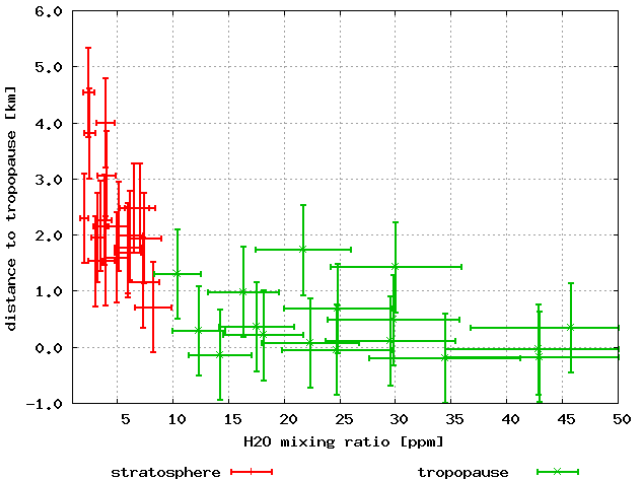

Fig. 2. H_2O-mixing ratio plotted versus distance to the tropopause. A decrease in mixing ratio with increasing distance to the tropopause is visible, which is due to mixing of relative moist air from the tropopause cold point with drier stratospheric air from above.

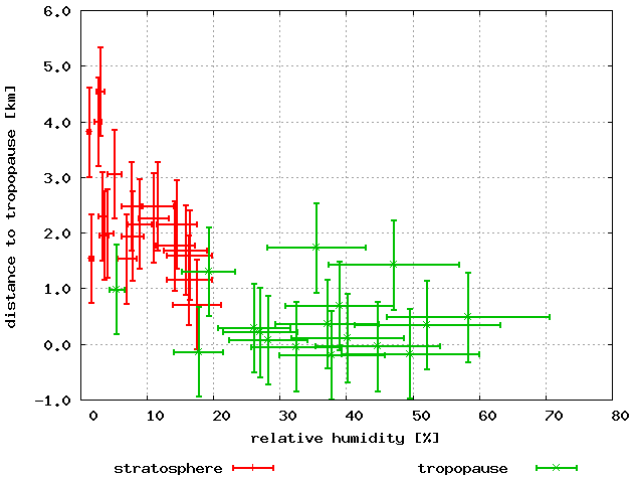

Fig. 3. Relative humidity plotted versus distance to the tropopause. As the relative humidity decreases with distance above the tropopause, the decreasing water vapor mixing ratio must be due to mixing of moist air from the tropopause level with dry stratospheric air.

the stratospheric samples taken in August all have $\upsilon \geq 5$ ppm. Thus the October samples are likely to contain air from the dehydrated stratosphere, where mixing ratios as low as 2 ppm have been observed by various instruments (e.g. SAGE-II, Chiou et al. (1997), data for September, October, November; HALOE, H_2O data at http://haloedata.larc.nasa.gov/; Stone et al., 2001).

Note that low water vapor mixing ratios alone may not be sufficient to classify air parcels as stratospheric, since the Antarctic upper trosposphere can also reach levels as low as 2 ppm in winter (Kelly et al., 1991). The temperature/water correlation is the more stringent criterion, and is supported by the independent information about the distance to the tropopause (see Table 1).

To exclude the possibility of condensation leading to the observed decrease of water vapor mixing ratio above the tropopause, the relative humidity of the samples is plotted versus the distance to the tropopause in Fig. 3. For the calculation of relative humidity, the mixing ratio and the pressure at sample altitude have to be known. However, there are no pressure data available on the C-17 flights, as its navigation solely depends on the global positioning system (GPS). The pressure is calculated from the GPS-altitude, assuming an atmospheric scale height of H=8.0±0.5 km. The relative humidity can be calculated from the altitude z, the mixing ratio υ and the vapor pressure over ice E_s at the ambient temperature T:

$$f = \frac{\upsilon \cdot 1023\,\mathrm{hPa} \cdot \exp(-z/H)}{E_s(T)} \cdot 100\% \qquad (3)$$

The error of f stems from the error of the mixing ratio of 20%, and an assumed error of 7% from the estimation of H, so that $\Delta f/f$ has a total error of 21% by quadratic addition.

Relative humidity is below 60% for all samples. Furthermore, a decrease in relative humidity with increasing distance to the tropopause is evident, so that a condensation process can be ruled out. This shows that the decreasing mixing ratio of water vapor across the tropopause is due to mixing with dry stratospheric air. That all samples at tropopause height have a relative humidity below 100% may be due to a difference in thermal and dynamical tropopause. Measurements from the MOZAIC project indicate a uniform probability for finding a specific relative humidity below 100% in the troposphere, whereas in the stratosphere the probability for finding a specific relative humidity decreases exponentially with increasing relative humidity (Gierens et al., 1999). In this context, values below 60% do not appear unreasonable.

4.2 δ^{18}O-data

No clear dependence of δ^{18}O on the distance to the tropopause is evident in the data. This might be because the data are taken over a latitude range of ∼30 degrees. However, the data are too sparse to allow for detailed analysis of both latitude and altitude dependence in a two-dimensional plot.

Figure 4 shows a plot of δ^{18}O versus H_2O mixing ratio. For the tropopause samples with υ>10 ppm, no correlation between mixing ratio and δ^{18}O can be found. The isotopic composition of water vapor here is δ^{18}O∼−60‰, with a rather wide data range between −90...−30‰. This high variability is likely caused by meteorology and different transport histories of the air parcels, as will be explained later.

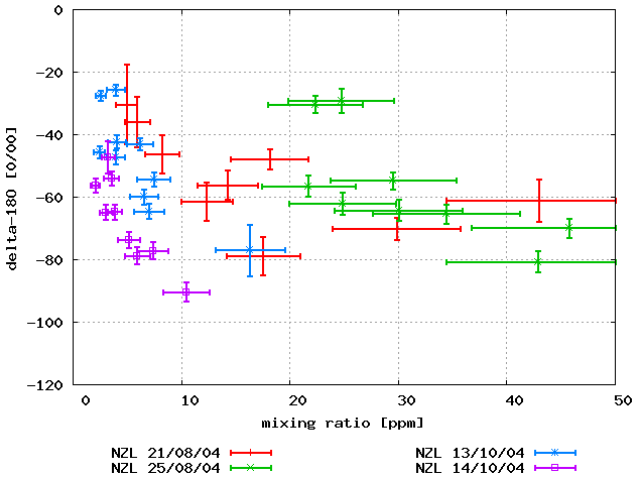

Fig. 4. δ^{18}O plotted versus mixing ratio. The tropopause samples with υ>10 ppm show no tight correlation between mixing ratio and δ^{18}O, whereas the individual stratospheric datasets appear to share a common slope (see Fig. 5).

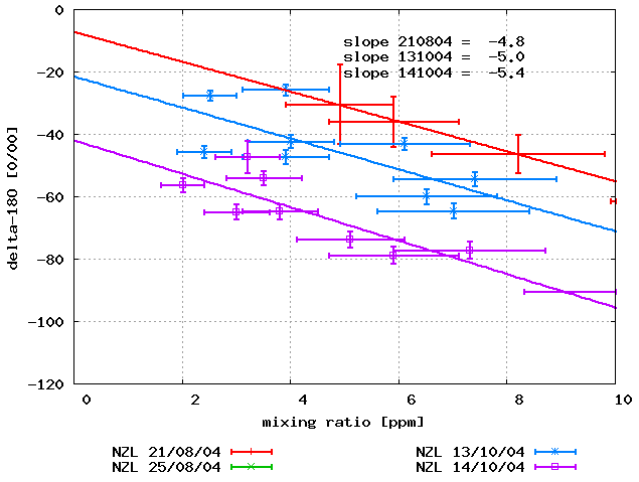

Fig. 5. δ^{18}O of the stratospheric samples plotted versus mixing ratio. A tight relationship between mixing ratio and isotopic composition is evident; the individual datasets share the same slope.

However, an interesting effect is seen in the relationship between mixing ratio and isotopic composition for υ<10 ppm. Figure 5 shows only the stratospheric datapoints. A linear regression line is fit to the data of each individual flight. Though there is an offset between the lines, the slopes are similar with roughly −5‰/ppm. This means that the linear fits for the three flights with stratospheric samples do not intersect at a common point. This is intriguing, since we would have expected a common stratospheric mixing point. However, at minimum stratospheric mixing ratios of ∼3 ppm, δ^{18}O varies between −60... − 20‰ for the three different flights. Since the photochemical lifetime of water vapor in the lower stratosphere in the order of years (Bechtel and Zahn, 2003), photochemistry can not produce such variation. The dependence of δ^{18}O on the mixing ratio seen in Fig. 5 must therefore be due to mixing of water vapor from the extratropical tropopause with older stratospheric air. However, our data show that this stratospheric water vapor reservoir can not have a uniform isotopic composition. Unfortunately, no other supporting data is available on the transfer flights to characterize the origin of the stratospheric mixing end members.

4.3 Δ^{17}O-data

In order to discuss the Δ^{17}O anomaly of water vapor, a three-isotope plot of δ^{17}O versus δ^{18}O is shown in Fig. 6. The water samples generally show mass-dependent fractionation, closely following the MDF-law as defined in Eq. (2). In order to investigate the small deviations from the MDF-law, a plot of Δ^{17}O versus the water vapor mixing ratio is shown in Fig. 7. The analytical precision in Δ^{17}O is around 0.35‰ for sample sizes corresponding to ∼50 ppm mixing ratio or more. However, most of the sample amounts collected during the flights are smaller (see Fig. 2). This results in the higher scatter seen in Fig. 7. The whole set of Δ^{17}O-data has a mean of 0.13‰, a standard deviation of 0.95‰, and a standard error of 0.16‰. A deviation from zero can therefore not be concluded at a statistically significant level. It is of interest to note that Δ^{17}O shows no dependence on either mixing ratio, distance to the tropopause or altitude. Therefore, our measurements shows that close to the tropopause Δ^{17}O must be ≤2‰. This can have important consequences.

The photochemical base model of Bechtel and Zahn (2003) suggests a maximum anomaly of roughly Δ^{17}O=6‰ in the stratosphere. However, there are three additional oxygen isotope exchange rates which could alter the Δ^{17}O anomaly of water vapor significantly, though their reaction rates can only be estimated at an upper limit so far. If oxygen isotope exchange (HO_2+O_2, OH+O_2) proceeds with the estimated upper limit, the anomaly vanishes to −0.6‰. This model result stems from either the small intrinsic mass anomaly that originates from different three-isotope slopes for different MDF processes mentioned in the introduction, or is a numeric effect, since doubly substituted molecules (e.g. $H^{18}O^{17}O$) are not included in the model. On the other hand, isotope exchange via the unknown reaction rate of NO_2+H_2O drastically increases the anomaly to ∼28‰, if this rate is considered at the assumed upper limit of $2.3 \cdot 10^{-13} \cdot \exp(-2100/T)$ cm^3 s^{-1} (Lyons, 2001). If there are no further mechanisms that can remove Δ^{17}O from water vapor (like the exchange reactions of HO_x with O_2), our data suggest that NO_2+H_2O exchange is negligible, i.e. at least one order of magnitude slower than the so far suggested upper limit.

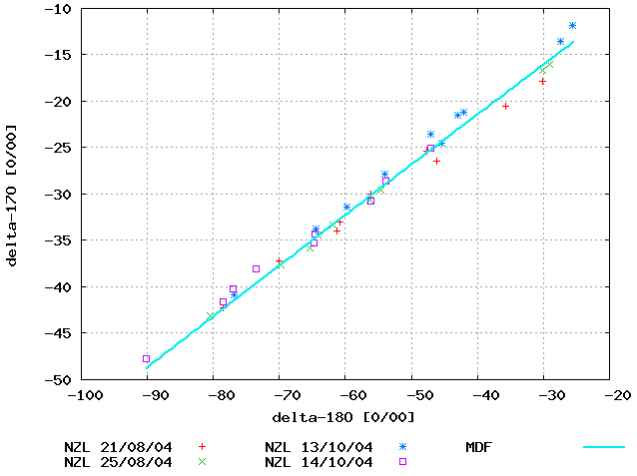

Fig. 6. Three-isotope plot of δ^{17}O versus δ^{18}O. The line represents mass-dependent fractionation that is defined as Δ^{17}O=0‰ (see Eq. 2). The samples only deviate slightly from mass-dependent fractionation, as further shown in Fig. 7.

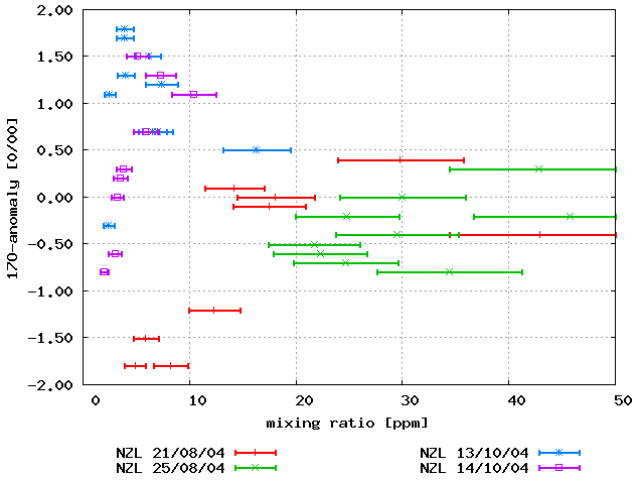

Fig. 7. Δ^{17}O plotted versus water vapor mixing ratio. No significant oxygen isotope anomaly can be deduced from the data. The error of Δ^{17}O is ∼0.35‰ for the larger samples with υ∼50 ppm, and increases with lower mixing ratios. Therefore, a significant deviation from zero is not expected.

4.4 Transport and photochemistry in the stratosphere

As has been shown above, the plot of H_2O mixing ratio versus temperature indicates that relative moist air from the tropopause with υ∼10 ppm mixes with dry stratospheric air. Since the isotopic composition of water vapor at the tropopause is determined by the precipitation and temperature history of the air parcel, it displays a high variability due to meteorology. This is also evident in data from lower latitudes (Webster and Heymsfield, 2003) on δD and δ^{18}O of water vapor. Our data indicate that this meteorological variability can penetrate into the layer of the lowermost stratosphere. A "tape recorder" effect like the one seen by Mote et al. (1996) in the stratosphere can not be seen at high latitudes, since this is a region of stratospheric subsidence.

There are two possible explanations for the low water vapor mixing ratios of ∼3 ppm encountered in some of the samples. First, the stratospheric air that mixes with the tropospheric air could have entered the stratosphere over the tropical tropopause, which is a known source for deeply dehydrated air. This air could then be transported quickly to higher latitudes in the lowermost stratosphere (Tuck et al., 1997). Second, dehydration at the cold temperatures in the polar vortex during Antarctic winter could be the cause for the low mixing ratios observed. The concentration data may support this scenario, since during the flights in August the observed water vapor mixing ratios were generally higher. In October, at a time where dehydration should be severe (Stone et al., 2001), the measured water vapor mixing ratios reached the lowest values.

We can examine the isotope data to further investigate the source of the stratospheric air. As water vapor crosses the tropical tropopause, strong depletions of around δ^{18}O=−130‰ on average are expected (Webster and Heymsfield, 2003; Johnson et al., 2001; Dinelli et al., 1991; Rinsland et al., 1991). This air can then be transported to higher latitudes either slowly as part of the Brewer-Dobson circulation, or more quickly just above the tropopause. In the latter case, there is not enough time for photochemical processing to produce the high δ^{18}O values observed. However, Zahn et al. (1998) have also observed rather high δ^{18}O values above the mid latitude tropopause. This is interpreted by Zahn (2001) by fast transport in warm conveyor belts and ice lofting, which can lead to significantly smaller depletions than pure Rayleigh condensation processes. Also in the tropics, Webster and Heymsfield (2003) show a large variability, with often only very small depletions, which must be due to ice lofting. It is possible that similar processes explain high δ^{18}O values we observe at higher latitudes. Fast transport processes would also be able to explain the absence of MIF in the samples. Water vapor from the tropical tropopause will have Δ^{17}O close to zero, since its isotopic composition is determined by condensation and evaporation processes, which fractionate in a mass-dependent way. However, in this case it is not clear which mechanisms can dehydrate the stratospheric air to the low mixing ratios we observed at the high southern latitudes.

The second possibility is slow transport through the central stratosphere as part of the global Brewer-Dobson circulation. As has been shown in the model of Bechtel and Zahn (2003), in this case water can undergo enough photochemical processing to reach rather high δ^{18}O values. However, if transport occured through the central stratosphere ∼1−2 ppm H_2O from methane oxidation would be produced in addition to the ∼3−4 ppm transported into the tropical

stratosphere. The low mixing ratios observed indicate that this requires a further dehydration process which has removed some of the H_2O (e.g. the cold polar vortex).

What would happen to water vapor from the polar vortex? First, the vortex contains air originating from the central stratosphere. This air should have a H_2O mixing ratio of about 5−6 ppm, and an isotopic composition of $\delta^{18}O$=−25...0‰ seems likely for old stratospheric air. Assuming 50% dehydration at 190 K and a fractionation constant of ∼28‰ of the (liquid) condensate versus the vapor (Majoube, 1971), a simple Rayleigh distillation yields $\delta^{18}O \sim -43 ... -19$‰, which is within the range observed in the 2...4 ppm data. This scenario, though speculative, can explain both the observed mixing ratios and the $\delta^{18}O$ data. However, present photochemical models (Lyons, 2001; Bechtel and Zahn, 2003) imply that old stratospheric water vapor should have a significant $\Delta^{17}O$ anomaly due to interaction of HO_x with NO_x, $O(^1D)$ and O_3. This is not supported by our data. It should be noted that key isotope exchange rates in the models are only known as an upper limit. Including or excluding these reactions in the models has very strong effects on the magnitude of the anomaly in water vapor. If the stratospheric air sampled has been processed through the Brewer-Dobson circulation, our data imply that either isotope exchange of OH, HO_2 with O_2 is not negligible, or that oxygen isotope transfer from NO_x is slower than assumed by Bechtel and Zahn (2003). Further information on the key exchange rates is needed before $\Delta^{17}O$ data can be used to examine stratospheric transport and photochemical processes.

A more detailed analysis of the water vapor mixing ratio and isotope data presented in this paper requires analysis of the condensation history of the sampled air parcels, e.g. by using computer based trajectories and microphysical modeling. An ideal model would combine both transport across the tropopause and photochemistry, but such a model is not yet available. Also, for characterization of air masses and atmospheric processes it would be very useful to make simultaneous measurements of other stratospheric and tropospheric tracers in future experiments.

4.5 Comparison to other measurements

Only two datasets of the oxygen isotopic composition of water vapor are available for comparison with the new observations. Webster and Heymsfield (2003) have measured mean values of $\delta^{17}O$=−6±30‰, $\delta^{18}O$=−179±72‰ in water vapor near the tropical tropopause level. As the tropical tropopause is located much higher than the polar tropopause and has far lower temperatures, smaller depletions are expected at mid and high latitudes. This is true for $\delta^{18}O$ measured in this work, which shows a $\delta^{18}O$ minimum of −90‰. The $\delta^{17}O$ measured here is with −48‰ significantly lower than the mean observed by Webster and Heymsfield (2003).

The mean results of Webster and Heymsfield (2003) indicate an isotope anomaly of $\Delta^{17}O$=98‰. However, individual errors in their measurements are large, and since errors in $\delta^{17}O$ and $\delta^{18}O$ in optical measurements are not necessarily correlated the anomaly is most likely not statistically different from zero. As the region in which their data was obtained is a zone of convective updraft, the isotopic composition should mainly be controlled by condensation and mixing processes, which are both not believed to generate a $\Delta^{17}O$ anomaly.

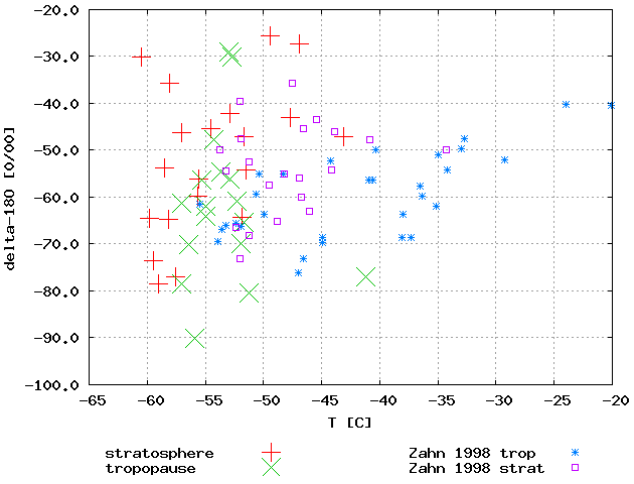

Fig. 8. Comparison of the $\delta^{18}O$ data with measurements by Zahn et al. (1998) as a plot versus temperature. As the measurements in this work were mostly taken at or above tropopause level, the correlation with temperature is stronger in the tropospheric samples of Zahn et al. (1998) than for this work. Above the tropopause, the data from Zahn et al. (1998) show the same behavior as the data presented here: high variability and a trend towards higher δ-values.

The data published in this work with $|\Delta^{17}O|$<2‰ are much more precise than any other data published before and improve the limit of $\Delta^{17}O$ by almost two orders of magnitude. Only with this precision the existence and magnitude of an isotope anomaly can be meaningfully investigated. The error in $\Delta^{17}O$ for the measurements with the new analytical system is smaller than the quadratic error of the individual $\delta^{17}O$, $\delta^{18}O$ measurements. This is because the errors imposed upon the measurements by handling of the sample in the analytical system are mass-dependent, and cannot lead to mass independently fractionated oxygen.

The second appropriate dataset is the one given by Zahn et al. (1998) from measurements mainly below tropopause height at northern mid to high latitudes. The $\delta^{18}O$ data are shown in Fig. 8 as plot versus sampling temperature. A depletion in $\delta^{18}O$ with decreasing temperature can be seen in the tropospheric samples down to −55°C, which is explained in a modified Rayleigh condensation model by Zahn (1995). Zahn et al. (1998) also found some H_2O samples of stratospheric origin, as identified by the high stratospheric O_3 values which were measured simultaneously. The stratospheric data of Zahn et al. (1998) are enriched in heavy isotopologues versus the tropospheric measurements. This is interpreted as

intrusions of stratospheric air by Zahn et al. (1998). The data presented in this work extend the isotopic range of stratospheric water vapor given by Zahn et al. (1998).

5 Conclusions

The isotope data presented here is the most precise dataset of combined δ^{18}O and Δ^{17}O measurements of water vapor in the stratosphere so far. The precision obtained is sufficient to study the natural changes of the isotopic composition of water vapor in the stratosphere.

The measurements of water vapor mixing ratios clearly indicate a mixing between dry stratospheric air and relatively moist air from the tropopause. With the available data, we suggest two different origins for the sampled stratospheric water: either fast transport in the lower stratosphere, or slow transport in the Brewer-Dobson circulation followed by dehydration in the polar vortex. Both scenarios still have open questions. The fast transport pathway can not explain the low water vapor mixing ratios observed, whereas water vapor transported through the central stratosphere should display mass independent fractionation according to present models. However, the magnitude of this mass independent fractionation still needs to be further investigated. Information about isotopic fractionation and exchange rates is not sufficient to distinguish between the two pathways based on the isotope data.

Further analysis of δ^{18}O and Δ^{17}O requires more knowledge on key isotope exchange rates and new computer models, which should include both two-dimensional transport, cloud microphysics and photochemistry.

Acknowledgements. We would like to thank NIWA Wellington, Antarctica NZ and the US Antarctic Program for their logistical support. This project received funding from the International Bureau of the DLR, project NZL02/001 and from the German BMBF in the AFO 2000C program, project ISOSTRAT. We would like to thank D. Lowe and G. Brailsford for their personal assistance, without which this project would never have been successful, and A. Zahn for valuable discussion.

Edited by: D. Grainger

References

Abbas, M., Guo, J., Carli, B., Mencaraglia, F., Bonetti, A., Carlotti, M., and Nolt, I.: Stratospheric O_3, H_2O and HDO Distributions From Balloon-Based Far-Infrared Observations, J. Geophys. Res., 92, 8354–8364, 1987.

Bechtel, C. and Zahn, A.: The isotope composition of water vapour: A powerful tool to study transport and chemistry of middle atmospheric water vapour., Atmos. Chem. Phys. Discuss., 3, 3991–4036, 2003,
SRef-ID: 1680-7375/acpd/2003-3-3991.

Carli, B. and Park, J.: Simultaneous Measurement of Minor Stratospheric Constituents With Emission Far-Infrared Spectroscopy, J. Geophys. Res., 93, 3851–3865, 1988.

Chiou, E., McCormick, M., and Chu, W.: Global water vapor distribution in the stratosphere and upper troposphere derived from 5.5 years of SAGE II observations (1986–1991), J. Geophys. Res., 102, 19 105–19 118, 1997.

Dinelli, B., Carli, B., and Carlotti, M.: Measurement of Stratospheric Distributions of $H_2^{16}O$, $H_2^{18}O$, $H_2^{17}O$ and $HD^{16}O$ From Far Infrared Spectra, J. Geophys. Res., 96, 7509–7514, 1991.

Dinelli, B., Lepri, G., Carlotti, M., Carli, B., Mencaraglia, F., Ridolfi, M., Nolt, I., and Ade, P.: Measurement of the isotopic ratio distribution of $HD^{16}O$ and $H_2^{16}O$ in the 20–38 km altitude range from far-infrared spectra, Geophys. Res. Lett., 24, 2003–2006, 1997.

Forster, P. M. d. F. and Shine, K.: Assessing the climate impact of trends in stratospheric water vapor, Geophys. Res. Lett., 29, 10-1–10-4, 2002.

Franz, P.: The Isotopic Composition of Water Vapor in the Upper Troposphere/Lower Stratosphere Region: Modeling, Analysis and Sampling, Ph.D. thesis, University of Heidelberg, http://www.ub.uni-heidelberg.de/archiv/5295, 2005.

Franz, P. and Röckmann, T.: A new continuous flow isotope ratio mass spectrometry system for the analysis of δ^2H, δ^{17}O and δ^{18}O of small (120 μg) water samples in atmospheric applications, Rapid Communications in Mass Spectrometry, 18, 1429–1435, 2004.

Gierens, K., Schumann, U., Helten, M., Smit, H., and Marenco, A.: A distribution law for relative humidity in the upper troposphere and lower stratosphere derived from three years of MOZAIC measurements, Ann. Geophys., 17, 1218–1226, 1999,
SRef-ID: 1432-0576/ag/1999-17-1218.

Guo, J., Abbas, M., and Nolt, I.: Stratospheric $H_2^{18}O$ distribution from far infrared observations, Geophys. Res. Lett., 16, 1277–1280, 1989.

Johnson, D. G., Jucks, K. W., Traub, W. A., and Chance, K. V.: Isotopic composition of stratospheric water vapor: Measurements and photochemistry, J. Geophys. Res.-Atmospheres, 106, 12 211–12 217, 2001.

Kelly, K., Tuck, A., and Davies, T.: Wintertime asymmetry of upper tropospheric water between the Northern and Southern Hemispheres, Nature, 353, 244–247, 1991.

Kirk-Davidoff, D. B., Hintsa, E. J., Anderson, J. G., and Keith, D. W.: The effect of climate on ozone depletion through changes in stratospheric water vapour, Nature, 402, 399–401, 1999.

Kuang, Z., Toon, G., Wennberg, P., and Yung, Y.: Measured HDO/H_2O ratios across the tropical tropopause, Geophys. Res. Lett., 30, 25-1–25-4, 2003.

Lyons, J. R.: Transfer of Mass-Independent Fractionation in Ozone to other Oxygen-containing Radicals in the Atmosphere, Geophys. Res. Lett., 28, 3231–3234, 2001.

Majoube, M.: Fractionnement en ^{18}O entre la glace et la vapeur d'eau, J. Chim. Phys. Physiochim. Biol., 68, 625–636, 1971.

Meijer, H. and Li, W.: The Use of Electrolysis for accurate δ^{17}O and δ^{18}O Isotope Measurements in Water, Isotopes Environ. Health Stud., 34, 349–369, 1998.

Miller, M. F.: Isotopic fractionation and the quantification of ^{17}O anomalies in the oxygen three-isotope system: an appraisal and geochemical significance, Geochimica et Cosmochimica Acta,

66, 1881–1889, 2002.

Mote, P. W., Rosenlof, K. H., McIntyre, M. E., Carr, E. S., Gille, J. C., Holton, J. R., Kinnersley, J. S., Pumphrey, H. C., III, J. M. R., and Waters, J. W.: An atmospheric tape recorder: The imprint of tropical tropopause temperatures on stratospheric water vapor, J. Geophys. Res., 101, 3989–4006, 1996.

Moyer, E., Irion, F., Y. L.Yung, and Gunson, M.: ATMOS stratospheric deuterated water and implications for troposphere-stratosphere transport, Geophys. Res. Lett., 23, 2385–2388, 1996.

Oltmans, S., Vömel, H., Hofmann, D., Rosenlof, K., and Kley, D.: The increase in stratospheric water vapor from balloonborne, frostpoint hygrometer measurements at Washington, D.C., and Boulder, Colorado, Geophys. Res. Lett., 27, 3453–3456, 2000.

Pollock, W., Heidt, L. E., Lueb, R., and Ehhalt, D. H.: Measurement of stratospheric water vapor by cryogenic collection, J. Geophys. Res., 85, 5555–5568, 1980.

Rinsland, C., Gunson, M., Foster, J., Toth, R., Farmer, C., and Zander, R.: Stratospheric profiles of heavy water vapor isotopes and CH_3D from analysis of the ATMOS Spacelab 3 infrared solar spectra, J. Geophys. Res., 96, 1057–1068, 1991.

Röckmann, T., Grooß, J., and Müller, R.: The impact of anthropogenic chlorine, stratospheric ozone change and chemical feedbacks on stratospheric water, Atmos. Chem. Phys., 4, 693–699, 2004,
SRef-ID: 1680-7324/acp/2004-4-693.

Rosenlof, K.: Transport Changes inferred from HALOE water and methane measurements, J. Meteorol. Soc. Japan, 80, 831–848, 2002.

Rosenlof, K., Oltmans, S., Kley, D., III, J. R., Chiou, E., Chu, W., Johnson, D., Kelly, K., Michelsen, H., Nedoluha, G., Remsberg, E., Toon, G., and McCormick, M.: Stratospheric water vapor increases over the past half-century, Geophys. Res. Lett., 28, 1195–1198, 2001.

Rosenlof, K. H.: Seasonal cycle of the residual mean meridional circulation in the stratosphere, J. Geophys. Res., 100, 5173–5191, 1995.

Stenke, A. and Grewe, V.: Simulation of stratospheric wate vapor trends: impact on stratospheric ozone chemistry, Atmos. Chem. Phys., 5, 1257-1272, 2005,
SRef-ID: 1680-7324/acp/2005-5-1257.

Stone, E. M., Tabazadeh, A., Jensen, E., Pumphrey, H. C., Santee, M. L., and Mergenthaler, J. L.: Onset, extent, and duration of dehydration in the Southern Hemisphere polar vortex, J. Geophys. Res., 106, 22 979–22 989, 2001.

Stowasser, M., Oelhaf, H., Wetzel, G., Friedl-Vallon, F., Maucher, G., Seefeldner, M., Trieschmann, O., Clarmann, T., and Fischer, H.: Simultaneous measurements of HDO, H_2O, and CH_4 with MIPAS-B: Hydrogen budget and indication of dehydration inside the polar vortex, J. Geophys. Res., 104, 19 213–19 225, 1999.

Tuck, A., Baumgardner, D., Chan, K., Dye, J., Elkins, J., Hovde, S., Kelly, K., Loewenstein, M., Margitan, J., May, R., Podoslke, J., Proffitt, M., Rosenlof, K., Smith, W., Webster, C., and Wilson, J.: The Brewer-Dobson circulation in the light of high altitude in situ aircraft observations, Q. J. Met. Soc., 123, 1–69, 1997.

Webster, C. R. and Heymsfield, A. J.: Water Isotope Ratios D/H, $^{18}O/^{16}O$, $^{17}O/^{16}O$ in and out of Clouds Map Dehydration Pathways, Science, 302, 1742–1745, 2003.

Young, E. D., Galy, A., and Nagahara, H.: Kinetic and equilibrium mass-dependent isotope fractionation laws in nature and their geochemical and cosmochemical significance, Geochimica et Cosmochimica Acta, 66, 1095–1104, 2002.

Zahn, A.: Der Tracertransport in der Tropopausenregion, Ph.D. thesis, Universität Heidelberg, 1995.

Zahn, A.: Constraints on 2-Way Transport across the Arctic Tropopause Based on O_3, Stratospheric Tracer (SF_6) Ages, and Water Vapor Isotope (D, T) Tracers, J. Atmos. Chem., 39, 303–325, 2001.

Zahn, A., Barth, V., Pfeilsticker, K., and Platt, U.: Deuterium, oxygen-18, and tritium as tracers for water vapour transport in the lower stratosphere and tropopause region, J. Atmos. Chem., 30, 25–47, 1998.